

## Research Paper

# A homogenization equation for the small strain stiffness of gap-graded granular materials

X.S. Shi<sup>a,b,\*</sup>, Jiayan Nie<sup>b,c</sup>, Jidong Zhao<sup>b</sup>, Yufeng Gao<sup>a</sup>

<sup>a</sup> Geotechnical Research Institute, College of Civil and Transportation Engineering, Hohai University, Nanjing, China

<sup>b</sup> Department of Civil and Environmental Engineering, Hong Kong University of Science and Technology, Clearwater Bay, Kowloon, Hong Kong

<sup>c</sup> State Key Laboratory of Water Resources and Hydropower Engineering Science, Wuhan University, Wuhan, China

## ARTICLE INFO

## Keywords:

Small strain stiffness  
Particle shape  
Volume average scheme  
Granular materials  
Homogenization theory

## ABSTRACT

Sandstone usually disintegrates into gap-graded granular materials with a matrix-sustained structure due to weathering factors. This paper presents an investigation on the small strain stiffness of this type of granular materials based on Discrete Element Method (DEM) simulations. Our numerical results indicate the percentage of sliding contact is negligibly small within the small strain range, and the small strain stiffness of fines is well consistent with the widely recognized Hardin's equation. Both findings confirm the validity of DEM simulations on the study of small strain response of granular materials. The simulation results are further analyzed based on mixture theory. A structure variable is introduced to correlate with the evolution of inter-aggregates structure. This variable is found to increase with the volume fraction of coarse aggregates but is rather independent of the confining stress and the initial void ratio of the fine matrix. Based on the insights drawn from DEM simulations, a homogenization equation is proposed for the small strain stiffness of gap-graded granular soils to reproduce the small strain stiffness of gap-graded materials observed in our numerical simulations and is further validated by laboratory test data from the literature. The equation can be conveniently incorporated into classical elastoplastic models to model gap-graded granular materials.

## 1. Introduction

Gap-graded soils are widely deposited worldwide, e.g., the sand-fine mixtures in marine deposits (e.g., [60,67]) and dredging activities (e.g., [8,15]). As a typical gap-graded soils, rock-soil mixtures prevail in landslides and weathered areas (e.g., [47,79,48,44,40,59]). The mixtures are induced by weathering factors and further accumulation under gravity or flow [4,62,16,31,11]. The structure of gap-graded soils can be described by two possible types [48,52]: a matrix-sustained structure with aggregates floating in the matrix, and an aggregates-sustained structure when contacts between aggregates prevail. The fine content is usually beyond the “transitional fine fraction” in intensely weathered areas [72,12,5], and the gap-graded granular soils have a matrix-sustained structure. This type of fine-coarse mixtures has been widely used worldwide as construction materials in engineering projects, and their deformation is crucial for assessing the workability of these geo-structures.

Granular materials typically exhibit a semi-elastic behavior within a small strain range [29,39,9]. As reported by Clayton [10], the strain levels around well-designed geotechnical structures such as retaining

walls and foundations, are generally small, therefore, small strain stiffness is usually adopted for studying soils surrounding geo-structures. The values of small strain stiffness can be measured either using direct approach (e.g., the local LVDT) or indirect ones (e.g., resonant column tests). The consistency of the results relies on the sample preparation and measuring accuracy [7]. Additionally, the behavior of phases in gap-graded soils cannot be distinguished using the mentioned laboratory testing methods. The DEM becomes appealing in analyzing the small strain behavior of granular soils, since contacts and contact forces between grains can be easily tracked through a monotonous loading process, and state dependent variables of each phase can also be determined from contact properties [75,71,56,74,78]. This provides further insight to constitutive modeling.

The small strain stiffness of fine-coarse mixtures has been well documented in the literature, (e.g., [65,22,19,2,46,57,20]). However, most of previous studies focus on gap-graded materials with a large coarse fraction (usually higher than 60%), which is not suitable for intensely weathered sandstones. Moreover, only empirical equations based on laboratory works are available for description of small strain stiffness (e.g., [25]). Actually, the small strain stiffness of gap-graded

\* Corresponding author at: Geotechnical Research Institute, College of Civil and Transportation Engineering, Hohai University, Nanjing, China.

E-mail addresses: [qingsongsaint@gmail.com](mailto:qingsongsaint@gmail.com) (X.S. Shi), [njiayan@ust.hk](mailto:njiayan@ust.hk) (J. Nie), [jzhao@ust.hk](mailto:jzhao@ust.hk) (J. Zhao).

soils cannot be well described using these empirical equations (such as Hardin's equation), since the overall stiffness relies on the two factors: (1) the behavior of fine matrix, (2) a homogenization equation representing the influence of the inter-aggregate structure on the overall properties. In this study, a homogenization equation based on mixture theory will be further proposed to bridge the local and overall behavior of gap-graded materials, followed by validation based on data from literature. This equation can be conveniently incorporated into classical elastoplastic models.

## 2. State dependent variables of gap-graded granular materials

A gap-graded granular material consists typically of fine particles and incompressible aggregates. The constitutive relationship of this type of binary mixture can be analyzed within the homogenization theory, with the fine particles and void space being treated as the deformable matrix and the stiff aggregates being the coarse inclusions [51]. The coarse aggregates can be assumed to be randomly distributed within the matrix due to natural disintegration process [52]. In this case, small strain properties of the mixtures are controlled by the matrix and inter-aggregate skeleton which is related to the volume fraction of the coarse inclusions.

The structure of gap-graded granular materials is homogeneous on a macroscale due to random distributions of coarse aggregates in the fine matrix. Therefore, the state dependent variables of each phase and the overall values can be well defined and computed from numerical results. Two assumptions are made in the study: (1) No macro pores exist in the inter-aggregate space. Obviously, this assumption may be valid for intense weathered sandstones, but may not be suitable in case of a relatively large coarse fraction [55,63,37,52], (2) The coarse aggregates are much stiffer than the deformable matrix (usually two orders of magnitude higher), therefore, the deformation of coarse aggregates is assumed to be negligible ([36,35]). The total volume of a Representative Elementary Volume (denoted as RVE) of gap-graded soils is partitioned into three parts: the solid volume of fine particles,  $V_f$ ; the volume of void space,  $V_v$ ; and the solid volume of coarse aggregates,  $V_a$ . The volume fraction of coarse aggregates, defined as the ratio of the volume of aggregates to the overall volume, is given as

$$\phi_a = \frac{V_a}{V_v + V_a + V_f} \quad (1)$$

Due to extremely high stiffness of aggregates, the volume change of RVE can be regarded identical to that of the matrix. For a given coarse fraction, the volume fraction increases with rising stress level. It can reasonably bridge between the overall state variables and those of the constituents. Therefore, it is widely used in mixture theory to homogenize state variables, e.g., stresses and strains. It can be formulated as follows:

$$\phi_a = \frac{e_m - e}{e_m + e_m e} \quad (2)$$

with  $e_m$  being the void ratio of fine matrix, and  $e$  being the overall void ratio of gap-graded materials. The void ratio of the matrix is a function of the overall value of gap-graded materials:

$$e_m = \left( 1 + \frac{\psi_a \rho_f}{(1 - \psi_a) \rho_a} \right) e \quad (3)$$

where  $\rho_a$  and  $\rho_m$  are the densities of coarse aggregates and fine particles, respectively;  $\psi_a$  is the mass fraction of coarse aggregates. Note that Eq. (3) is derived from the conservation of the masses and volumes of each phase of the gap-graded materials. For a given initial state, the overall void ratio  $e$  depends uniquely on the current overall volumetric strain of the gap-graded materials  $\varepsilon_v$ :

$$e = (1 + e_0) \exp(-\varepsilon_v) - 1 \quad (4)$$

where  $e_0$  is the overall initial void ratio of gap-graded materials. The

current strain  $\varepsilon_v$  can be computed from the change of size of a specimen in a numerical simulation. Substitution of Eqs (3) and (4) into Eq. (2), the volume fraction of coarse aggregates can be obtained.

Nonhomogeneous structure between the phases induces a non-uniform stress distribution (Harshin, 1983; [14,13,50]). It is recognized that the variables defined based on volume fraction scheme provide satisfactory descriptions of the mechanical behavior of gap-graded materials [61,52]. Therefore, the stresses are estimated by the Love's equation and the volume average scheme [45]:

$$\sigma'_{ij}{}^{(m)} = \frac{1}{V_v + V_f} \sum_{c \in V_v + V_f} f_i^c d_j^c \quad (5a)$$

$$\sigma'_{ij}{}^{(a)} = \frac{1}{V_a} \sum_{c \in V_a} f_i^c d_j^c \quad (5b)$$

$$\sigma'_{ij} = \frac{1}{V_v + V_f + V_a} \sum_{c \in V_v + V_f + V_a} f_i^c d_j^c \quad (5c)$$

where  $\sigma'_{ij}$  is the overall stress tensor of gap-graded materials,  $\sigma'_{ij}{}^{(m)}$  and  $\sigma'_{ij}{}^{(a)}$  are the stress tensors of the matrix and aggregates, respectively;  $d_j^c$  and  $f_i^c$  are the branch vector between two adjacent particles and the contact force vector, respectively. The summations in Eqs. (5a)–(5c) are performed over contacts of all particles within corresponding volumes.

## 3. DEM simulations

DEM simulations are performed to measure the small strain stiffness of gap-graded mixtures. Both the fine particles and coarse aggregates in a gap-graded soil are modelled as rigid particles with an extremely high shear stiffness. The coarse aggregates are created randomly within the fine matrix. There are many factors influencing the stiffness of gap-graded granular materials, including the coarse fraction of aggregates, the particle size distribution and particle shape of fines and aggregates [67,43,53,51,15,52]. It is recognized that the initial state significantly affects the stiffness of geo-materials (e.g., [3,42,4,66,33,18,68]). Therefore, the influence of initial void ratio of the matrix in gap-graded materials should be distinguished. To this end, three main factors are considered in DEM simulations: (1) the fraction of coarse aggregates, (2) the initial state of fine matrix, and (3) the shape of coarse aggregates. The generation of DEM packings will be first presented, followed by a triaxial loading process.

### 3.1. Generation of DEM specimens

In this study, cubic specimens are generated by DEM as approximation of REV for a gap-graded granular material (side length  $\approx 4.0 \times 10^{-2}$  m). The coarse inclusions (spherical or natural aggregates) are randomly distributed in each specimen. Three different types of particles are used for the generation of DEM specimens (Fig. 1): (1) Fine particles with a diameter of  $1.5 \times 10^{-3}$  m, (2) spherical coarse aggregates with a diameter of  $6.0 \times 10^{-3}$  m, and (3) natural coarse aggregates with the same volume of solid as the spherical coarse aggregates. The natural aggregates are created by clumping small spherical particles ([76,77]). Three descriptors are used for the shape characteristic of the natural aggregates [64], with aspect ratio, mean curvature and sphericity of 0.828, 0.641 and 0.869, respectively: the aspect ratio reflects the proportions of aggregates; mean curvature represents variations at corners; and sphericity is the ratio of specific area between the spherical aggregates and the natural aggregate. 123 small particles are used to create a single natural aggregate (see Fig. 1).

In order to reflect the influence of coarse fraction and state of fine matrix, DEM specimens with two different initial state of fine matrix and four various volume fractions of coarse aggregates are tested. As listed in Table 1, a denser one with a void ratio of (0.614–0.618) and an

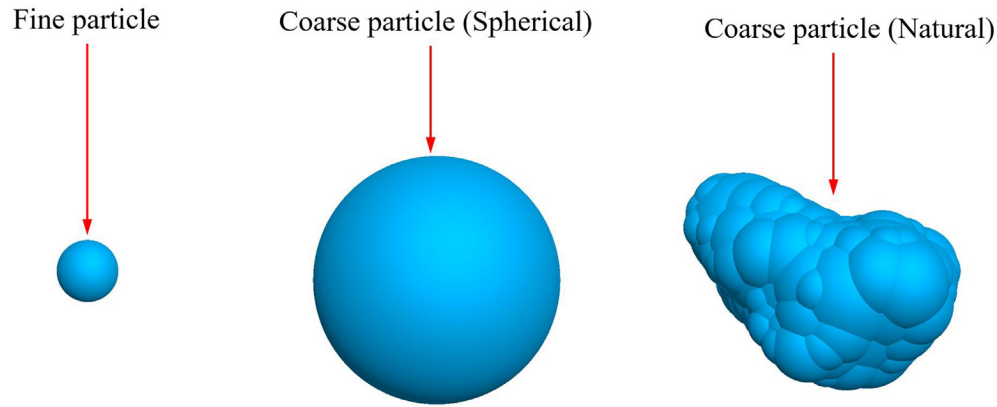


Fig. 1. Geometry of three types of particles used in discrete element simulation.

intermediate one (0.650–0.653) are adopted. The specified volume fractions of coarse aggregates of DEM specimen are 4.9–5.1%, 9.7–9.8%, 18.9–19.0%, and 35.5–36.3%, respectively. For natural aggregates, an additional simulation with a volume fraction of 27.6% is performed. Note that the void ratio of fine matrix and the volume fraction of aggregates show a slight variation at different stress levels.

The coarse aggregates are created randomly within the fine matrix. A two-step procedure is used in this study for the creation of coarse aggregates, according to the following algorithm: (1) coarse aggregates (the size is larger than the desired values) are created within a representative volume surrounded by rigid walls. The centroid is randomly generated, and there may be overlaps between the aggregates. (2) The inter-aggregate structure is perturbed due to possible overlaps between the aggregates, and the algorithm for the motion follows the laws in DEM (Cundall and Strack, 1979). After a semi-equilibrium state being reached, the aggregates will be reduced to the desired size, and the position of each aggregates is recorded. In this case, the gap between coarse aggregates can be user-defined, which should exceed the order of the size of fine particles.

The created aggregates are inserted into the fine matrix to obtain a geometric model for the DEM simulations. The fine particles with centroids inside the coarse aggregates will be deleted from the REV. This intersection induces excessive forces, which disturbs the original structure of the gap-graded specimens. As a result, contacts may occur between the coarse aggregates, and the void ratio of fine matrix increases. The overall void ratio of gap-graded materials after mixing process is given in Table 1. Note that the overall void ratio is higher than that predicted by “ideal” mixing model [70]. “ideal” denotes that the two types of materials are fully mixed with no disturbance of the

fine matrix. This phenomenon coincides with the observations in previous work (e.g., [63,54,30,70]) that the ideal mixing model underestimates the porosity of binary mixtures due to non-ideal mixing. Only the DEM specimens with mass fraction of coarse aggregates below 53% is investigated in this work, which is consistent with the intense weathered sandstones in field cases [79,52,5,6]. For an extremely high coarse fraction, the fine mass may not be sufficient to fill the inter-aggregates space, leading to macro-pores in gap-graded materials.

### 3.2. Numerical simulations

The numerical simulations in this study are performed based a commercial DEM code, Itasca PFC3D (version 5.0). Details of the specimens for DEM simulations are presented in Table 1. Specimens with different coarse fractions are prepared according to the procedures described in the previous section. In this study, a simplified Hertz-Mindlin contact model with a constant shear stiffness in conjunction with the Coulomb’s friction law is used to describe the inter-particle interactions [34]. The model is defined by two parameters: shear modulus  $M$  and Poisson’s ratio  $\nu$  of two contacting particles. The normal contact stiffness  $k_n$  and shear stiffness  $k_t$  are calculated as

$$k_n = \frac{2M}{1 - \nu} \sqrt{\frac{r_1 r_2}{r_1 + r_2}} \delta_n \quad (6a)$$

$$k_t = \frac{4M}{2 - \nu} \sqrt{\frac{r_1 r_2}{r_1 + r_2}} \delta_n \quad (6b)$$

where  $\delta_n$  is the contact overlap which is a function of normal force, and  $r_1$  and  $r_2$  are radii of two contacting particles. The Hertz-Mindlin contact model has been adopted in many previous simulations (e.g.,

Table 1  
Details of the samples for numerical simulation.

| Notation                        | $\psi_a$ (%) | $\sigma_3$ (kPa) | $e$               | $\phi_a$ (%) | $N_f$  | $N_a$ |
|---------------------------------|--------------|------------------|-------------------|--------------|--------|-------|
| Series-1 (Spherical aggregates) | 0.0          | 50,100,200       | 0.618,0.617,0.614 | 0.0          | 20,000 | 0     |
|                                 | 8.1          |                  | 0.588,0.587,0.584 | 5.1          | 18,954 | 26    |
|                                 | 15.4         |                  | 0.564,0.563,0.561 | 9.8          | 17,948 | 51    |
|                                 | 28.9         |                  | 0.518,0.517,0.515 | 19.0         | 15,929 | 101   |
|                                 | 52.3         |                  | 0.443,0.442,0.440 | 36.3         | 11,781 | 202   |
| Series-2 (Spherical aggregates) | 0.0          | 50,100,200       | 0.653,0.652,0.650 | 0.0          | 20,000 | 0     |
|                                 | 8.1          |                  | 0.633,0.631,0.630 | 4.9          | 18,968 | 26    |
|                                 | 15.6         |                  | 0.608,0.607,0.605 | 9.7          | 17,959 | 52    |
|                                 | 29.5         |                  | 0.564,0.562,0.561 | 18.9         | 15,893 | 104   |
|                                 | 53.1         |                  | 0.479,0.478,0.477 | 35.9         | 11,713 | 207   |
| Series-3 (Natural aggregates)   | 8.1          | 100              | 0.589             | 5.1          | 18,954 | 26    |
|                                 | 15.4         |                  | 0.566             | 9.8          | 17,954 | 51    |
|                                 | 28.8         |                  | 0.527             | 18.9         | 15,942 | 101   |
|                                 | 41.2         |                  | 0.493             | 27.6         | 13,912 | 152   |
|                                 | 51.9         |                  | 0.460             | 35.5         | 12,005 | 202   |
| Additional                      | 0.0          | 50,100,200       | 0.705,0.704,0.702 | 0.0          | 20,000 | 0     |

[1,41,73]).

Following the physical properties of quartz sands, the value of the Poisson's ratio, shear stiffness and density of the particles (both fines and coarse aggregates) are adopted as 0.15, 10 GPa and  $2.65 \times 10^3 \text{ kg/m}^3$ , respectively. Note that the solid density is magnified  $10^6$  times here to speed up the simulation, and a large fixed timestep ( $10^{-5}$ ) is set in the DEM simulation. At this timestep, the corresponding normalized unbalance force in our simulation has been found less than  $10^{-6}$ , which is small enough for the quasi-static analysis in this study. To prepare specimens with different densities for the pure fine matrix, the friction coefficient  $\mu$  is set to 0.01, 0.15, and 0.30, respectively, during the consolidation stage. After equilibrium is achieved at an initial consolidation stress of 10 kPa, the aggregates are inserted into the fine matrix, and the system is allowed to reach a new equilibrium state at the constant confining stress. The consolidation pressure is then gradually increased to a target value (50–200 kPa) by applying numerical servo-mechanism. Finally, a friction coefficient of 0.30 is assigned to the particles, and the specimens are compressed under a constant confining stress (50 kPa, 100 kPa and 200 kPa).

The overall deviatoric stress of the gap-graded soils can be computed from the homogenized stress tensor in Eq. (5). The principal strain variants are defined as the logarithm of the ratio of the current values to their initial ones. The overall shear stiffness of gap-graded soils  $G$  is calculated as

$$G = \frac{q}{3\varepsilon_s} \quad (7)$$

where  $q$  and  $\varepsilon_s$  are deviatoric stress and deviatoric strain, respectively. The change of stiffness with deviatoric strain for pure fine matrix is presented in Fig. 2. It shows that the stiffness is approximately constant before decreasing dramatically. This semi-elastic stiffness is denoted as the small strain stiffness. In this study, since we only focus on the small strain properties, the shear tests are stopped if the axial strain approaches  $10^{-5}$ .

The results of the overall small strain stiffness of the gap-graded materials with various coarse fractions are summarized in Fig. 3 in terms of stiffness and volume fraction of coarse aggregates. Both the void ratio of fine matrix and the coarse fraction affect the overall small strain stiffness. The overall small strain stiffness of gap-graded materials decreases with the void ratio of fine matrix. The change of overall small strain stiffness with the volume fraction depends critically on the void ratio of matrix. For gap-graded specimens with a lower void ratio of matrix (Series-1), the overall small strain stiffness shows a stable increase with increasing coarse fraction. However, it shows only a negligible increase in case of a higher void ratio of fine matrix (Series-2), and it even decreases for small coarse fractions. This is due to the combining effect of the initial state and the coarse fraction. Mixing process may disturb the structure of fine matrix, therefore, the mixture becomes loose and the stiffness decreases. However, the reinforcement

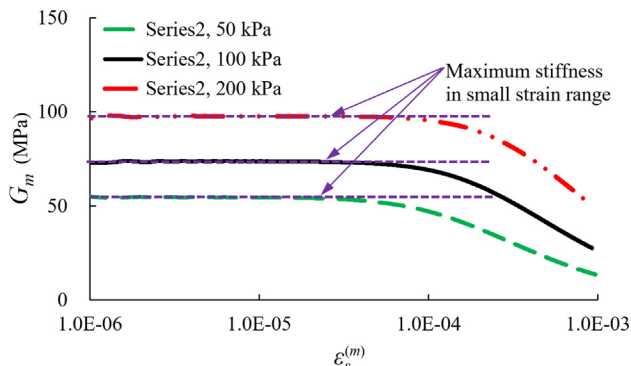


Fig. 2. Change of small strain stiffness with deviatoric strain for pure fine matrix.

of aggregates leads to an increase of the stiffness. The decrease of void ratio is dominated at low coarse fraction, hence the small strain stiffness decreases. With the increase of coarse fraction, the influence of reinforcement plays a more important role, leading to an increase of small strain stiffness decreases of mixtures. This is consistent with the laboratory data reported by Ruan et al. [46].

There are two probable mechanisms governing the small strain stiffness of gap-graded soils: (1) adding coarse aggregates may disturb the original structure of fine matrix, causing a decrease of the overall small strain stiffness; (2) The reinforcement of coarse inclusions due to partial contacts between coarse aggregates (arises from the random distribution of coarse inclusions) and “densified soil layer” between adjacent coarse aggregates (forms due to the gradual densification of fine particles) [28,15,52]. This induces an increase of the overall small strain stiffness. The combination of the above two mechanisms controls the change of small strain stiffness after adding coarse aggregates.

#### 4. Microscopic structure variables within small strain range

The small strain stiffness corresponds to the mechanical response of granular materials with neither significant plastic dissipation nor structure change. In this work, it equals the semi-constant stiffness within an axial strain of  $10^{-5}$ . The following microscopic structure variables will be analyzed to validate the assumption of negligible change of internal structure. These variables describe the contact properties, including the percentage of sliding contact, the coordination number, and the contact anisotropy. Since there are only a few contacts between coarse aggregates for strongly weathered gap-graded soils, three categories of contacts are considered in this study: fine-fine, fine-coarse, and the overall contacts.

The change of percentage of sliding contact is shown in Fig. 4. It is defined as the ratio of the number of sliding contacts to the number of total contacts. The percentage of sliding contact is extremely small (less than 0.05%) within a deviatoric strain of  $10^{-6}$ . It shows a slight increase afterwards, however, it is still below 0.6%. This indicates that the sliding of contact as well as the plastic dissipation are negligible within the small strain range.

Three coordination numbers (CN) are computed and their change in small strain range are summarized in Fig. 5, where the subscripts “t”, “ff” and “fa” denote the overall contact, fine-fine contact and fine-coarse contact, respectively. It is seen that the coordination numbers at different stress levels are approximately the same, and they seem to remain constant within the simulated strain range. Therefore, the coordination numbers for gap-graded specimens with a given coarse fraction can be approximated by a scalar, and their evolution against the volume fraction of coarse aggregates are shown in Fig. 6. The CN of overall contacts and fine-fine contacts decreases with the increasing coarse content, while the CN of fine-coarse contact shows a slight increase. The decrease of CN of fine-fine contact reveals a disturbance of fine matrix with adding of coarse inclusions, suggesting an increase of porosity and decrease of small strain stiffness of the fines.

The mechanical response of granular soils relies on the contact anisotropy. After Guo and Zhao [23], the overall contact anisotropy of gap-graded mixtures is defined as

$$\beta_t = \text{sign}(a_{ij}^c \sigma_{ij}') \sqrt{\frac{3}{2} a_{kl}^c a_{kl}^c} \quad (8)$$

with  $a_{ij}^c = \frac{15}{2} \phi_{ij}'$  being the second-order anisotropy tensors of contact.  $\phi_{ij}'$  is the deviatoric part of second-order anisotropy tensor  $\phi_{ij}$ :

$$\phi_{ij} = \frac{1}{N_c} \sum_{c \in V_f + V_a} n_i n_j \quad (9)$$

where  $N_c$  is the number of contact, and  $n_i$  is the unit vector along the normal direction of the contact plane. Analogously, the contact anisotropy of fine-fine contact and fine-coarse contact can be defined,

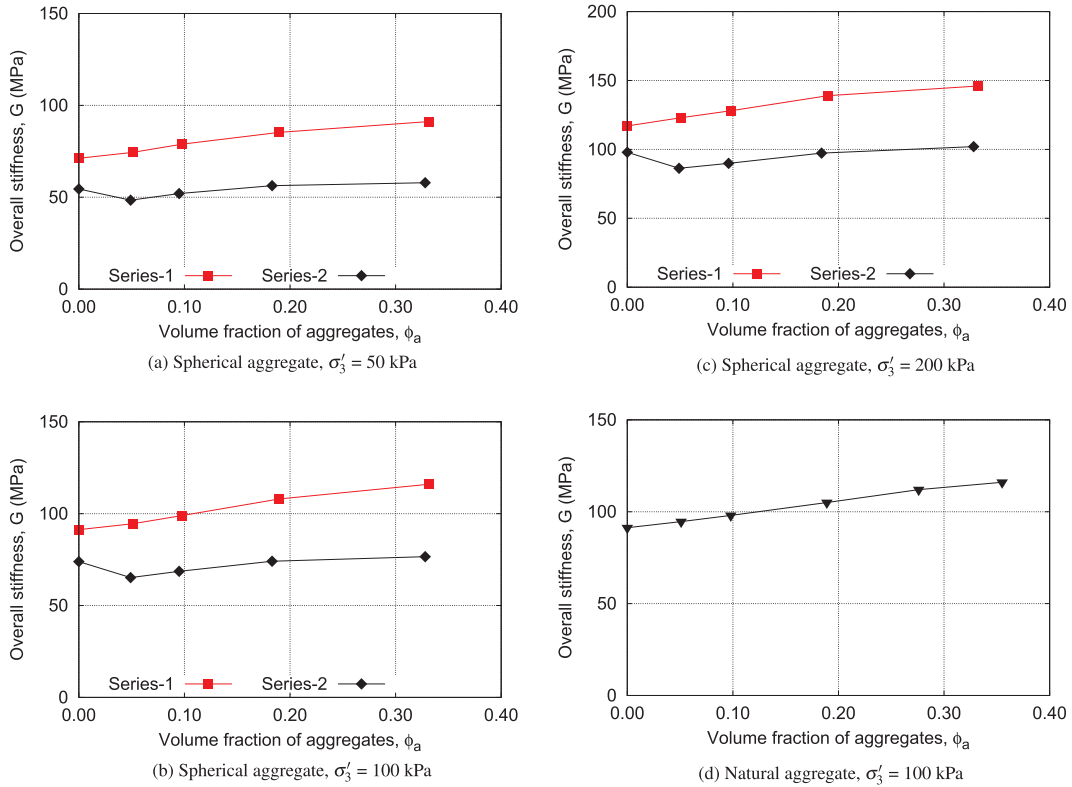


Fig. 3. Change of small strain stiffness with volume fraction of coarse aggregates at various stress levels.

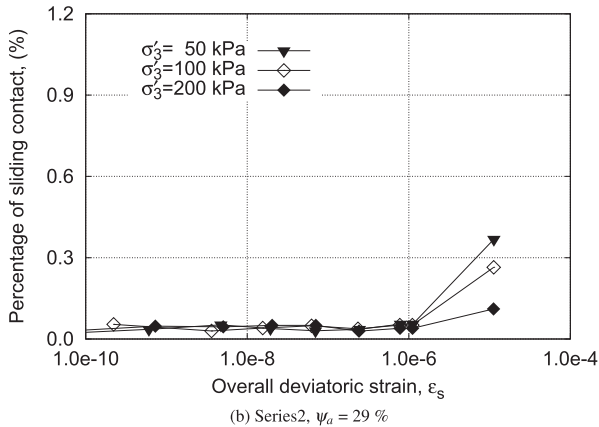
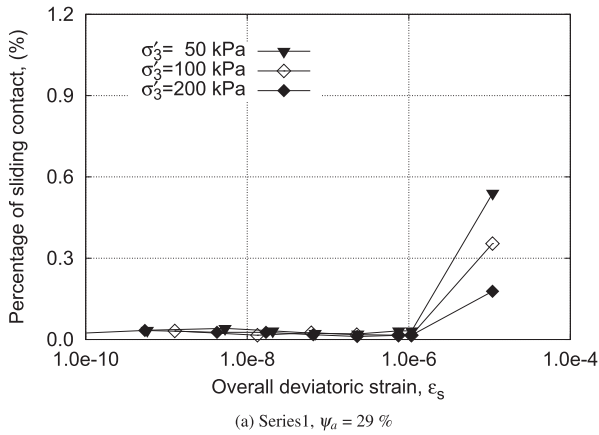


Fig. 4. Change of sliding of contacts with overall deviatoric strain.

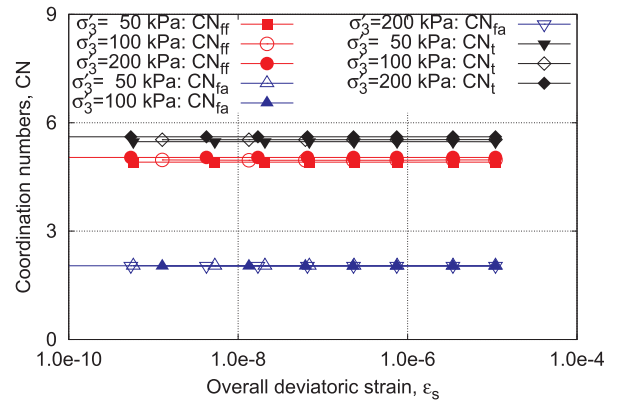


Fig. 5. Evolution of coordination number with overall deviatoric strain (Series1,  $\psi_a = 29\%$ ).

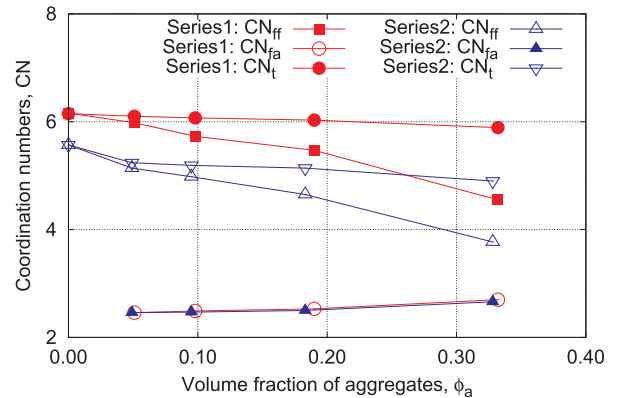


Fig. 6. Change of coordination number with volume fraction of aggregates ( $\sigma'_3 = 100$  kPa).

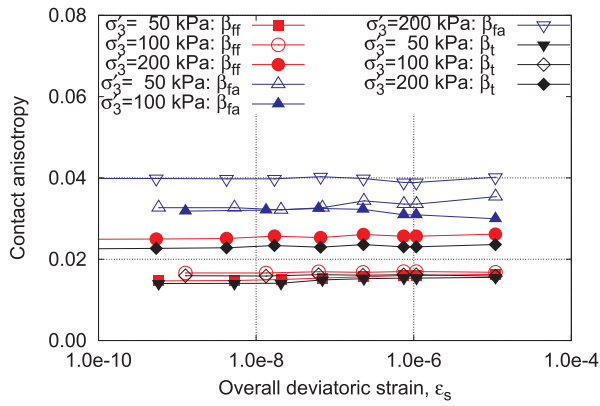


Fig. 7. Change of contact anisotropy with overall deviatoric strain (Series1,  $\psi_a = 29\%$ ).

denoted by the subscripts “ff” and “fa”, respectively. The results are summarized and presented in Fig. 7. Only the simulation of Series-1 with 29% coarse fraction is presented, since the results in all cases are similar. It is seen that the contact anisotropy in all three types of contacts is relatively small, and it remains almost unchanged within small strain regime. This indicates a negligible change of internal structure within the small strain loading regime. This is consistent with the structure of strong weathered residual soils. Some other researchers create the coarse aggregates and fines within a predefined space, the constituents adjust the internal structure till it reaches an equilibrium state. This mixing process may produce direct contacts between the aggregates, leading to a nonnegligible anisotropic structure even at low coarse fractions.

### 5. Analysis of small strain stiffness using homogenization approach

As noted by Shi and Yin [51], for a fine matrix reinforced by stiff inclusions, the overall stiffness of gap-graded materials can be computed based on the following consideration: (1) the stiffness of fine matrix in gap-graded soils, (2) a homogenization equation representing the influence of the inter-aggregate structure on the overall properties. In this section, a reference model will be selected for the small strain stiffness of the fines, and the change of inter-aggregate structure with coarse fraction will be investigated.

### 6. Reference model for the small strain stiffness of fine matrix

The small strain stiffness of fine granular materials is influenced by both soil structure (e.g. over-consolidation ratio, void ratio, gradation, structural anisotropy) and testing conditions (e.g. confining stress, stress anisotropy). Normally consolidated specimens with mono-disperse particles and isotropic structure are considered in this study. Focus will be placed upon the effect of void ratio and confining stress. In the literature, various empirical models have been proposed for estimating the small strain stiffness of granular materials (e.g., [24,25,58]). We adopt the following general form of Hardin’s relationship that has been widely used in past studies [65,19,22,46]

$$\frac{G_m}{\sigma_r} = f(e_m) \left( \frac{\sigma_3^{(m)}}{\sigma_r} \right)^n \quad (10)$$

where  $n$  is a model parameter for the matrix,  $\sigma_3^{(m)}$  is the effective confining stress of the fine matrix,  $\sigma_r = 100$  kPa is a reference stress, and  $f(e_m)$  denotes a function of the void ratio of the matrix. The following function has been proposed by Hardin and co-workers [25]:

$$f(e_m) = A e_m^{-\alpha} \quad (11)$$

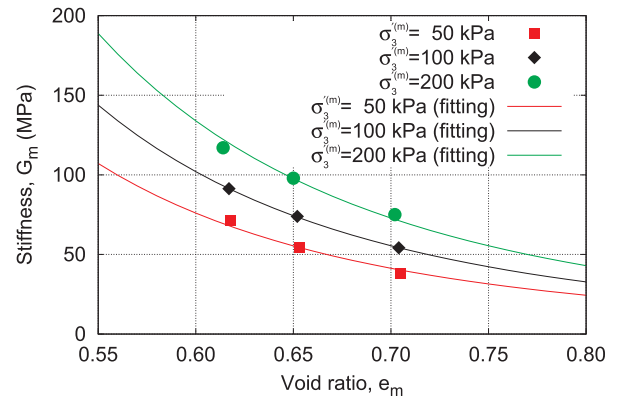


Fig. 8. Relationship between small strain stiffness and void ratio for pure fine particles.

where  $A$  and  $\alpha$  are model parameters for the fine matrix. The change of small strain stiffness with void ratio for pure fine particles is shown in Fig. 8 (the solid lines are fitting lines using power function Eq. (11),  $\alpha = 0.37$ ). The small strain stiffness decreases with the increase of void ratio, and their relationship can be well represented by a power law function. Calibration of model parameters based on a power function  $G_m$ - $e_m$  relationship is shown in Fig. 9, revealing an excellent regression. This confirms that DEM can be used for simulating the small strain response of granular materials. In the sequel, Hardin’s equation (Eqs (10) and (11)) will be used as the reference model for small strain stiffness of the pure fine matrix. The value of concave parameter  $\alpha$  is comparable to that reported by Goudarzy et al. [22], which is due to similarity in the value of parameters.

### 6.1. Homogenization model for gap-graded materials

Since we adopted the same physical properties of fine particles for specimens with pure fines and the ones containing coarse aggregates, it is reasonable to assume that the small strain stiffness of the matrix in gap-graded materials follows the reference model for the pure fine matrix (Eqs. (10) and (11)) regardless of the coarse fractions. Therefore, the small strain stiffness of the fine matrix in gap-graded materials can be calculated as

$$\frac{G_m}{\sigma_r} = A \left( 1 + \frac{\psi_a \rho_f}{(1-\psi_a)\rho_a} \right)^{-\alpha} \left( \frac{\sigma_3'}{\sigma_r} \right)^n e^{-\alpha \mu_\sigma^n} \quad (12)$$

where  $\sigma_3'$  denotes the overall stress of the gap-graded materials, which can be computed by Eq. (5c), a stress ratio  $\mu_\sigma$  is introduced to interpret the stress distribution in gap-graded materials. It is defined as the ratio of the average stress in the fine matrix and the overall stress in

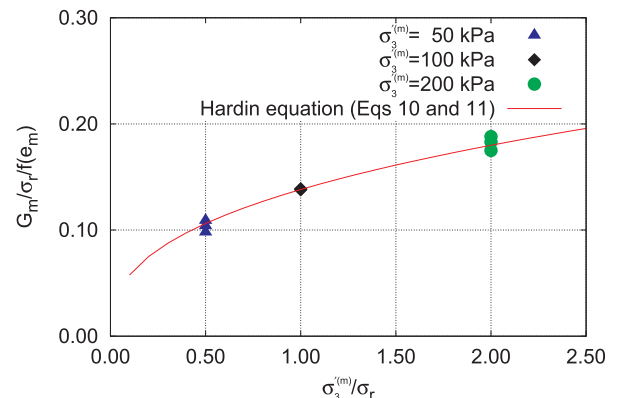


Fig. 9. Calibration of model parameters of Hardin’s relationship (Eqs (10) and (11)).

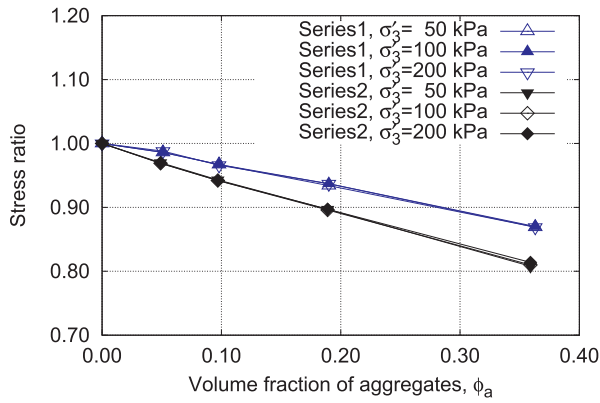


Fig. 10. Change of stress ratio with volume fraction of coarse aggregates.

gap-graded materials. The evolution of the stress ratio with different initial state of matrix, different confining stresses, and various coarse fractions stress are summarized in Fig. 10. It reveals that the stress ratio of the gap-graded materials is not sensitive to the confining stress level, however, it shows a continuous decrease with the increasing volume fraction of coarse inclusions. In addition, the stress ratio of gap-graded materials with a loose matrix is lower than that with a denser matrix. This reveals a different behavior from the sand-clay mixtures that the initial void ratio of matrix does not affect the stress distribution in the mixtures [51].

The structure of gap-graded materials can be bounded by two configurations within mixture theory: series model (lowest stiffness) and parallel model (highest stiffness). The weathering process induces a random distribution of coarse aggregates in the fine constituent, and the gap-graded mixture has a matrix-sustained structure. The shear stiffness of coarse aggregates is much higher than that of matrix, and the general “volume average approximation” concept cannot capture the overall small strain stiffness with a good accuracy. To this end, the following general homogenization relationship is proposed for the small strain stiffness of gap-graded materials:

$$\xi(\sigma_3, e_m, \phi_a) = \frac{G}{G_m} \quad (13)$$

where  $\xi$  is a structure variable, which is a function of the stress level, initial void ratio of the fine matrix and the volume fraction of coarse aggregates. It creates a bridge between overall small strain stiffness and that of the fine matrix. The small strain stiffness of fine matrix is calculated from Eq. (12), and the structure variable of gap-graded materials with various confining pressures and coarse fractions can be computed (per Eq. (13)). Fig. 11a shows the evolution of structure variable  $\xi$  against the volume fraction of coarse spherical aggregates. The structure variable increases with the increasing volume fraction of the coarse inclusions. However, it appears that this structure variable is rather independent of the confining stress as well as the initial void ratio of the fine matrix. Therefore, it is reasonable to assume that structure variable  $\xi$  depends only on the volume fraction of coarse aggregates.

The structure variable shows a highly nonlinear increase with the increasing coarse fraction. In the sequel, two limit cases are considered for the small strain stiffness of gap-graded materials: (1) the lower bound of structure corresponding to a negligible coarse fraction, and (2) the upper bound of the structure variable corresponding to the maximum coarse fraction. The overall void ratio of gap-graded soils is equal to that of the fine matrix if the coarse fraction is negligible, and the corresponding overall small strain stiffness is reduced to that of the matrix, i.e., the structure variable  $\xi = 1$ . The gap-graded material has a matrix-sustained structure until the coarse fraction approaches the minimum packing density of the aggregates [37]:

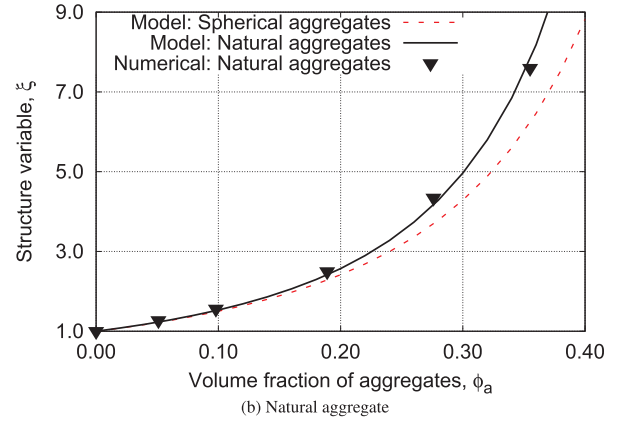
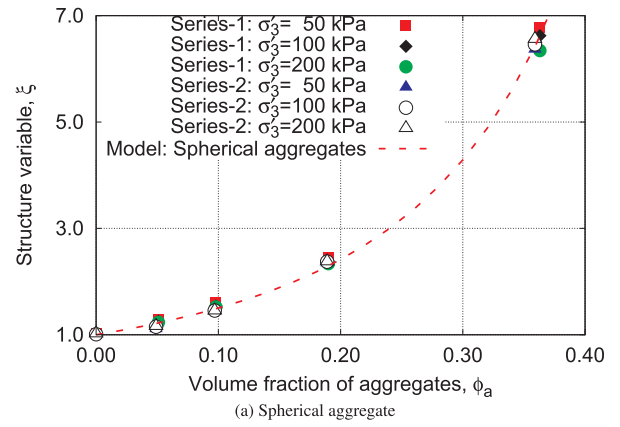


Fig. 11. Relationship between structure parameter and volume fraction of coarse aggregates.

$$\hat{\phi}_a = \frac{1}{1 + e^{a_{\max}}} \quad (14a)$$

where  $e^{a_{\max}}$  is the maximum void ratio of the coarse aggregates. A granular-sustained structure forms gradually with a further increase of coarse fraction. The gap-graded materials achieve the densest packing state when the coarse aggregate approaches its maximum packing density  $\hat{\phi}_a$ :

$$\tilde{\phi}_a = \frac{1}{1 + e^{a_{\min}}} \quad (14b)$$

The shear stiffness of the gap-graded soils becomes extremely high at the densest packing state, which is comparable to the stiffness of the solid aggregates. Therefore, the external loading is primarily sustained by the solid inter-aggregate skeleton, and the stress in the fine matrix becomes negligibly small. From Eq. (12), the small strain stiffness should be much smaller compared with the overall value. Therefore, the structure variable should meet the following requirements:

$$\phi_a \approx 0 \rightarrow \xi \approx 1; \text{ and } \phi_a \approx \tilde{\phi}_a \rightarrow \xi \approx +\infty \quad (15)$$

A tentative equation satisfying the above requirements can be expressed as follows:

$$\xi = \left( \frac{\tilde{\phi}_a}{\hat{\phi}_a - \phi_a} \right)^\eta \quad (16)$$

where  $\eta$  is a constant structure parameter for a given type of coarse aggregates. It controls the change of structure variable on the coarse fraction. Fig. 11b illustrates the change of structure variable  $\xi$  with the volume fraction of natural aggregates. It is seen that the structure variable is more sensitive to the coarse fraction than the gap-graded soils with coarse spherical aggregates. Substitution of Eq. (16) into Eq. (13) leads to

$$\log G = \log G_m + \eta \log \left( \frac{\tilde{\phi}_a}{\phi_a - \phi_a} \right) \quad (17)$$

Eq. (17) is a homogenization equation for the small strain stiffness of gap-graded materials. The overall stiffness is uncorrelated to the stiffness of the coarse aggregates, which is different from previous homogenization laws in classical mixture theory, e.g., Eshelby model [17], self-consistent method [27], Mori-Tanaka method [38], Lielens method [32], and the homogenization equation for lumpy soils [49]. The structure parameter  $\eta$  is affected by the nature of aggregates, e.g., particle shape and roughness of aggregates, and the particle size distribution of aggregates. However, the influence of coarse stress level, coarse fraction and the initial state is negligible. The value of structure parameter of natural aggregates is higher than that of spherical ones, and it also increases with the size ratio between aggregate and fines. Note that if significant fracturing of coarse aggregates occurs during the loading process, the structure parameter  $\eta$  will not be a constant. It is well recognized that sand particles in uniformly-graded granular soils may be broken into fine ones, especially at high stress levels. However, for the gap-graded granular mixtures, the aggregates are confined within the fine matrix. Hence, the stress in aggregates becomes more uniform. The confining stress from surrounding matrix prevents further breakage of the coarse aggregates [69].

## 7. Application of the proposed homogenization equation

Substitution of Eq. (12) into Eq. (17) gives a model for the small strain stiffness of gap-graded soils. There are one material parameter  $\eta$  for the homogenization law and three parameters for the small strain stiffness of the fine matrix,  $A$ ,  $\alpha$  and  $n$ . The structure parameter  $\eta$  can be calibrated from the small strain stiffness of gap-graded materials with a given fraction of coarse aggregates. The structure parameter depends on the inter-aggregate structure, which changes with the size and shape of coarse aggregates [26]. The other three parameters  $A$ ,  $\alpha$  and  $n$  can be calibrated from the relationship between small strain stiffness and the confining stress (or void ratio) of matrix. Four gap-graded granular materials are used for validation of the homogenization equation: two are the numerical gap-graded soils considered in this study, and the other two are from the literature [21,46]. Note that only the specimens with a coarse fraction less than 70% are adopted for validating the homogenization equation.

### 7.1. Materials in this study (Numerical simulation)

The gap-graded granular materials considered in the previous DEM simulations are mixtures of fine and coarse (rigid) particles, with the coarse particles (spherical aggregates or natural irregular aggregates) being the inclusions and fine particles being the matrix. The values of model parameters are listed in Table 2, and their calibration are shown in Figs. 8, 9 and 11. Comparisons between the model prediction and numerical simulations for the gap-graded materials are shown in Figs. 12 and 13. The comparison indicates that the overall small strain stiffness of gap-graded granular materials can be well reproduced by the proposed analytical model. Fig. 13 reveals that the proposed homogenization equation can reproduce the phenomenon of stiffness reduction (fraction of 9.7–9.8%) for gap-graded materials at a higher

**Table 2**  
Parameters for numerical simulation and laboratory data from literature.

| Sources                           | $\eta$ | $A$  | $\alpha$ | $n$  | $\tilde{\phi}_a$ |
|-----------------------------------|--------|------|----------|------|------------------|
| This study (Spherical aggregates) | 2.80   | 0.14 | 3.9      | 0.37 | 0.74             |
| This study (Natural aggregates)   | 2.45   | 0.14 | 3.9      | 0.37 | 0.63             |
| González-Hurtado and Newson [21]  | 0.64   | 0.13 | 3.7      | 0.55 | 0.74             |
| Ruan et al. [46]                  | 1.35   | 0.91 | 1.3      | 0.54 | 0.60             |

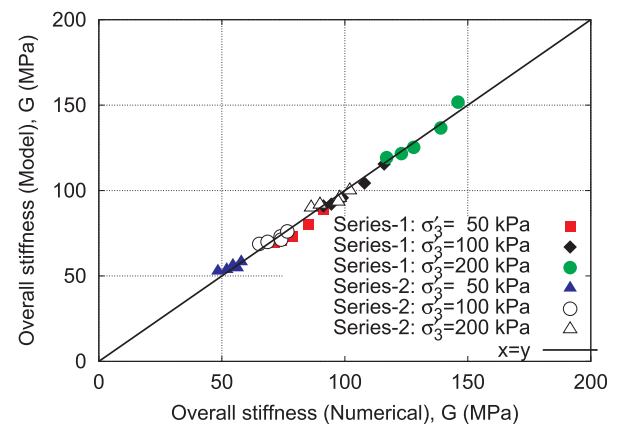


**Fig. 12.** Comparison between the numerical simulations and model predictions.

void ratio of matrix.

### 7.2. Materials from literature (Laboratory tests)

The gap-graded soils investigated by González-Hurtado and Newson [21] is a mixture of Ottawa silica sand (fine matrix) and spherical glass beads (coarse inclusions). The two phases have a similar mineralogical composition. The  $d_{50}$  of the fine particles and the coarse aggregates are 0.26 mm and 10.26 mm, respectively, leading to a size ratio of the coarse and fine particles at approximately 40. The maximum volume fraction of coarse aggregates corresponds to the densest packing state,  $\tilde{\phi}_a = 0.741$ . The particle densities of fine particles and aggregates are  $2.66 \times 10^3 \text{ kg/m}^3$  and  $2.50 \times 10^3 \text{ kg/m}^3$ , respectively. Five different mass fractions of coarse fractions of the gap-graded materials (0, 0.236, 0.455, 0.637 and 1.00) have been tested by González-Hurtado and Newson [21], and the corresponding volume fractions are 0, 0.168, 0.353, 0.541, and 1.00, respectively. The pure coarse aggregates are not used for validation of the homogenization equation. The specimens were prepared by air pluviation method and consolidated at three vertical stresses (60 kPa, 120 kPa and 240 kPa), before being sheared with a displacement rate of 0.02 mm/min. Torsional resonant frequency tests were performed for computing the small strain stiffness of the mixtures.

Another gap-graded material was examined by Ruan et al. [46]. A sandy soil from the coastal land in China was sieved with a mesh opening of 0.075 mm. The coarse particles larger than 0.075 mm were used as inclusions, and the fine ones were chosen as matrix. The average size ratio between the coarse aggregates and the fine particles is 2.85, with the  $d_{50}$  of the phases being 0.114 (coarse aggregates) and 0.040 (fine particles), respectively. The minimum void ratio of coarse aggregates is 0.662, hence the maximum volume fraction of coarse inclusions is  $\tilde{\phi}_a = 0.602$ . The density of granular particles for the coarse aggregates and fine particles are  $2.67 \times 10^3 \text{ kg/m}^3$  and  $2.72 \times 10^3 \text{ kg/m}^3$ , respectively. Three influencing factors, including the coarse fractions (0, 0.30, 0.50, 0.70, 0.80, 0.90, 1.00), stress levels (100 kPa, 200 kPa, 250 kPa, 300 kPa and 400 kPa), and relative density (35%, 50% and 60%), were examined. The cylinder specimens were prepared by the moist tamping method, and the compression tests were done using the dynamic triaxial apparatus.

The confining stress in the fine matrix is unknown (Eq. (12)) in the laboratory tests. However, this stress is related to the volume fraction of the coarse inclusions. Therefore, the confining stress in the matrix can be replaced by the overall confining stress, and its effect can be incorporated into the structure variable  $\xi$ . The values of model parameters are listed in Table 2. Note that the structure parameter  $\eta$  incorporates the effect of stress localization. Fig. 14 shows the change of structure parameter with the volume fraction of coarse inclusions, and Fig. 15 presents a comparison between the experimental data and

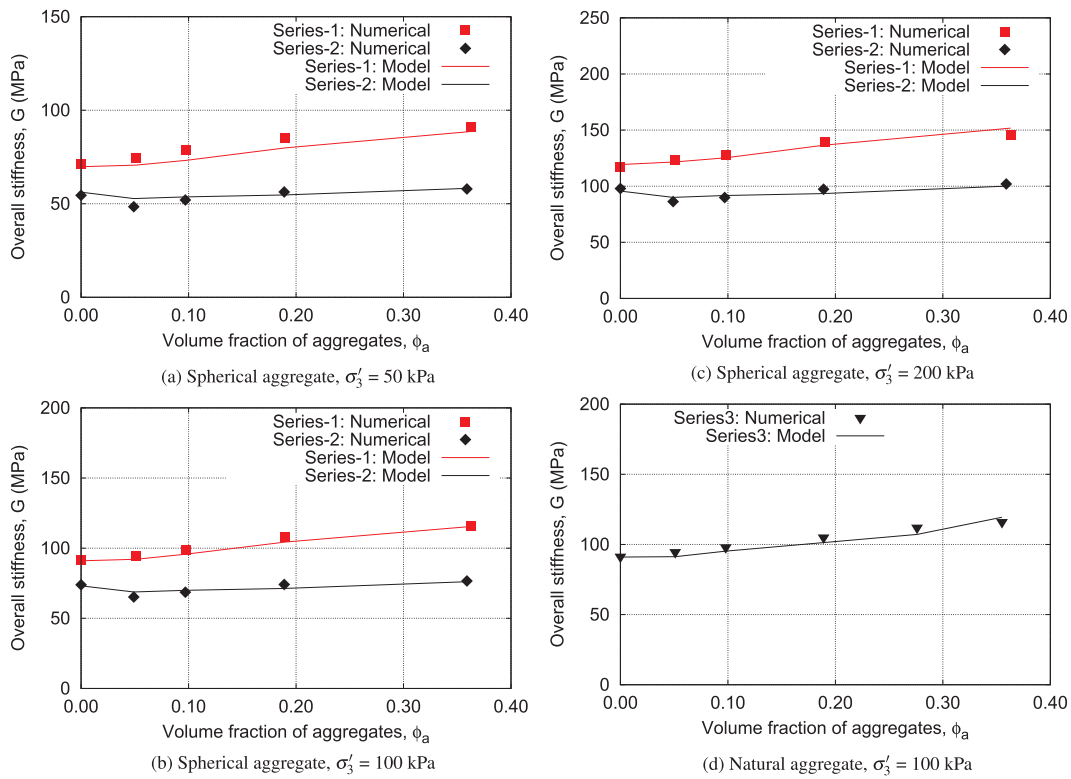
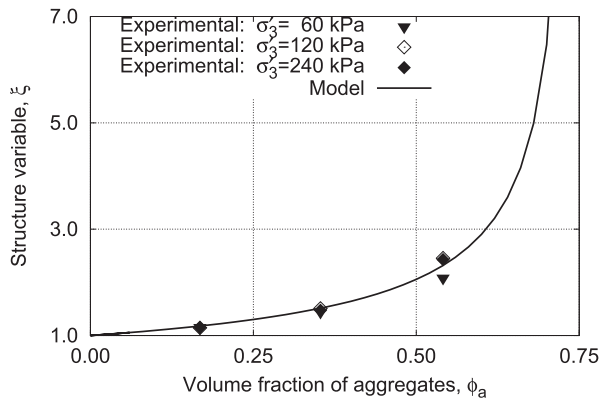
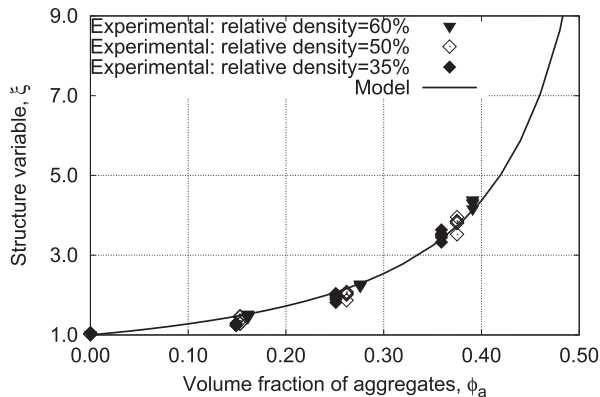


Fig. 13. Comparison between the numerical simulations and model predictions at different stress levels.



(a) Data from Gonzalez-Hurtado and Newson (2015)



(b) Data from Ruan et al. (2018)

Fig. 14. Relationship between structure parameter and volume fraction of coarse aggregates (data from literature).

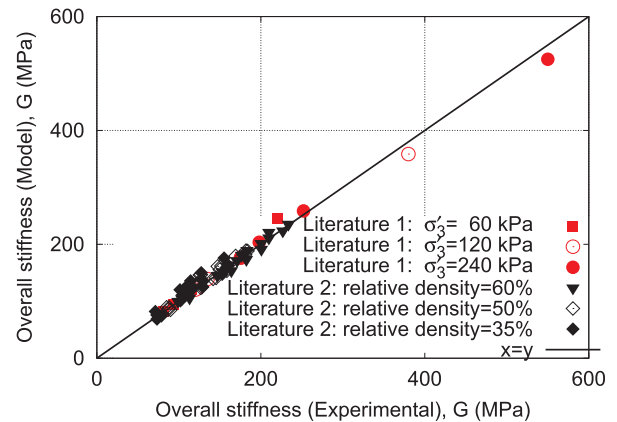


Fig. 15. Comparison between the numerical simulations and model predictions (data from literature 1: Gonzalez-Hurtado and Newson, 2015; data from literature 2: [46]).

analytical model predictions of the two gap-graded materials. Evidently, the model can well represent the effects of confining stress, relative density and coarse fraction as observed in the experimental tests.

### 8. Conclusions

Systematic DEM simulations have been performed to estimate the small strain stiffness of gap-graded materials. An analytical homogenization equation has been proposed based on volume fraction concept and mixture theory to estimate the small strain stiffness of gap-graded mixtures, with further comparisons with laboratory tests and numerical simulations. Major findings of the study are summarized as follows.

- (1) The small strain stiffness of a gap-graded material is affected by

both the void ratio of fine matrix and the coarse fraction. For gap-graded specimens with a lower void ratio of matrix, the overall small strain stiffness shows a continuous increase with increasing coarse fraction. However, it shows only a negligible increase in case of a higher void ratio of fine matrix.

- (2) Both the percentage of sliding of contact and the contact anisotropy are relatively small within the small strain range. Hence, the sliding of contact as well as the plastic dissipation are negligible. The small strain stiffness of sand matrix is well consistent with the widely recognized Hardin's equation. These confirm the feasibility of DEM for simulating the small strain response of granular materials.
- (3) A structure variable is introduced to represent the change of inter-aggregates structure. The structure variable increases with the increasing volume fraction of coarse inclusions, but shows an independence of the confining stress and the initial void ratio of the fine matrix.
- (4) The proposed analytical homogenization equation combined with Hardin's equation reproduces well small strain stiffness of gap-graded materials from both laboratory tests and numerical simulations.

### CRedit authorship contribution statement

**X.S. Shi:** Conceptualization, Methodology, Writing - original draft.  
**Jiayan Nie:** Software, Validation. **Jidong Zhao:** Conceptualization, Writing - review & editing. **Yufeng Gao:** Writing - review & editing.

### Declaration of Competing Interest

The authors declare that they have no known competing financial interests or personal relationships that could have appeared to influence the work reported in this paper.

### Acknowledgments

This study was partially supported by the National Natural Science Foundation of China (under Grant No. 51679207 and Grant No. 51908193) and the Research Grants Council of Hong Kong (under TBRS Grant No. T22-603/15N, RGC/GRF Grant No. 16210017, RGC/GRF Grant No. 16201419, and CRF Grant No. C6012-15G). The first author appreciates the funding support from VPRG Office of HKUST for his Research Assistant Professor (RAP) position. Zhijie Yu has run some DEM simulations to validate the findings of the study (results not presented).

### References

- [1] Barreto D, O'Sullivan C. The influence of inter-particle friction and the intermediate stress ratio on soil response under generalised stress conditions. *Granul Matter* 2012;14(4):505–21.
- [2] Bayat M, Ghalandarzadeh A. Stiffness degradation and damping ratio of sand-gravel mixtures under saturated state. *Int J Civil Eng* 2018;16(10):1261–77.
- [3] Burland JB. On the compressibility and shear strength of natural clays. *Géotechnique* 1990;40(3):329–78.
- [4] Chandler RJ. The Third Glossop Lecture: Clay sediments in depositional basins: the geotechnical cycle. *Q J Eng Geol Hydrogeol* 2000;33(1):7–39.
- [5] Chen WB, Borana L, Feng WQ, Yin JH, Liu K. Influence of matric suction on non-linear time-dependent compression behaviour of a granular fill material. *Acta Geotech* 2018;12.
- [6] Chen WB, Feng WQ, Yin JH, Borana L, Chen RP. Characterization of permanent axial strain of granular materials subjected to cyclic loading based on shakedown theory. *Constr Build Mater* 2018;54.
- [7] Chen WB, Yin JH, Feng WQ. A new double-cell system for measuring volume change of a soil specimen under monotonic or cyclic loading. *Acta Geotech* 2019;14(1):71–81.
- [8] Chu C, Wu Z, Deng Y, Chen Y, Wang Q. Intrinsic compression behavior of remolded sand-clay mixture. *Can Geotech J* 2017;54(7):926–32.
- [9] Clayton CRI, Heymann G. Stiffness of geomaterials at very small strains. *Géotechnique* 2001;51(3):245–55.
- [10] Clayton CRI. Stiffness at small strain: research and practice. *Géotechnique* 2011;61(1):5–37.
- [11] Cui YF, Jiang Y, Guo CX. Investigation of the initiation of shallow failure in widely graded loose soil slopes considering interstitial flow and surface runoff. *Landslides* 2019;16(4):815–28.
- [12] Cui YF, Zhou XJ, Guo CX. Experimental study on the moving characteristics of fine grains in wide grading unconsolidated soil under heavy rainfall. *J Mount Sci* 2017;14(3):417–31.
- [13] De Boer R. Trends in continuum mechanics of porous media 2006;Vol:18).
- [14] De Boer R, Ehlers W. On the problem of fluid and gas-filled elasto-plastic solids. *Int J Solids Struct* 1986;22(11):1231–42.
- [15] Deng Y, Wu Z, Cui Y, Liu S, Wang Q. Sand fraction effect on hydro-mechanical behavior of sand-clay mixture. *Appl Clay Sci* 2017;135:355–61.
- [16] Dittes M, Labuz JF. Field and laboratory testing of St. Peter sandstone. *J Geotech Geoenviron Eng* 2002;128(5):372–80.
- [17] Eshelby JD. The determination of the elastic field of an ellipsoidal inclusion, and related problems. *Proc Roy Soc A* 1957;241(1226): 376–396.
- [18] Gao Z, Zhao J, Li XS, Dafalias YF. A critical state sand plasticity model accounting for fabric evolution. *Int J Numer Anal Meth Geomech* 2014;38(4):370–90.
- [19] Giang PHH, Van Impe PO, Van Impe WF, Menge P, Haegeman W. Small-strain shear modulus of calcareous sand and its dependence on particle characteristics and gradation. *Soil Dyn Earthquake Eng* 2017;100:371–9.
- [20] Gong J, Liu J, Cui L. Shear behaviors of granular mixtures of gravel-shaped coarse and spherical fine particles investigated via discrete element method. *Powder Technol* 2019;353:178–94.
- [21] González-Hurtado J, Newson T. Measuring the small-strain elastic modulus of gap-graded soils using an effective-medium model and the resonant column apparatus. *Geo-Quebec 2015, Challenges from North to South*; 2015.
- [22] Goudarzy M, König D, Schanz T. Small strain stiffness of granular materials containing fines. *Soils Found* 2016;56(5):756–64.
- [23] Guo N, Zhao J. The signature of shear-induced anisotropy in granular media. *Comput Geotech* 2013;47:1–15.
- [24] Hardin BO. Dynamic versus static shear modulus for dry sand. *Mater Res Stand* 1965;5(5):232–5.
- [25] Hardin BO, Black WL. Sand stiffness under various triaxial stresses. *J Soil Mech Found Div* 1966:92.
- [26] Herle I, Gudehus G. Determination of parameters of a hypoplastic constitutive model from properties of grain assemblies. *Mech Cohesive-Friction Mater* 1999;4(5):461–86.
- [27] Hill R. A self-consistent mechanics of composite materials. *J Mech Phys Solids* 1965;13(4):213–22.
- [28] Jafari MK, Shafiee A. Mechanical behavior of compacted composite clays. *Can Geotech J* 2004;41(6):1152–67.
- [29] Jardine RJ, Symes MJ, Burland JB. The measurement of soil stiffness in the triaxial apparatus. *Géotechnique* 1984;34(3):323–40.
- [30] Kamann PJ, Ritzi RW, Dominic DF, Conrad CM. Porosity and permeability in sediment mixtures. *Groundwater* 2007;45(4):429–38.
- [31] Li Z, Gao Y, Wang K. Torsional vibration of an end bearing pile embedded in radially inhomogeneous saturated soil. *Comput Geotech* 2019;108:117–30.
- [32] Lielens G, Piroette P, Couniot A, Dupret F, Keunings R. Prediction of thermo-mechanical properties for compression moulded composites. *Compos A Appl Sci Manuf* 1998;29(1–2):63–70.
- [33] Mesri G, Vardhanabhuti B. Compression of granular materials. *Can Geotech J* 2009;46(4):369–92.
- [34] Mindlin RD, Deresiewicz H. Elastic spheres in contact under varying oblique forces. *J Appl Mech* 1953;20:327–44.
- [35] Mitchell JK, Soga K. *Fundamentals of soil behavior* Vol. 3. New York: John Wiley & Sons; 2005.
- [36] Monkul MM, Ozden G. Effect of intergranular void ratio on one-dimensional compression behavior. In: *Proceedings of international conference on problematic soils 2005*;Vol. 25, p. 27.
- [37] Monkul MM, Ozden G. Compressional behavior of clayey sand and transition fines content. *Eng Geol* 2007;89(3):195–205.
- [38] Mori T, Tanaka K. Average strain in matrix and average elastic energy of materials with misfitting inclusions. *Acta Metall* 1973;21(5):571–4.
- [39] Niemunis A, Herle I. Hypoplastic model for cohesionless soils with elastic strain range. *Mech Cohesive-friction Mater: An Int J Exp, Modell Comput Mater Struct* 1997;2(4):279–99.
- [40] Peng D, Xu Q, Liu F, He Y, Zhang S, Qi X, et al. Distribution and failure modes of the landslides in Heitai terrace, China. *Eng Geol* 2018;236:97–110.
- [41] Perez JL, Kwok CY, Senetakis K. Investigation of the micro-mechanics of sand-rubber mixtures at very small strains. *Geosynth Int* 2017;24(1):30–44.
- [42] Pestana JM, Whittle AJ. Compression model for cohesionless soils. *Géotechnique* 1995;45(4):611–31.
- [43] Peters JF, Berney IV ES. Percolation threshold of sand-clay binary mixtures. *J Geotech Geoenviron Eng* 2010;136(2):310–8.
- [44] Qin CB, Chian SC. Kinematic analysis of seismic slope stability with a discretisation technique and pseudo-dynamic approach: a new perspective. *Géotechnique* 2017;68(6):492–503.
- [45] Rothenburg L, Bathurst RJ. Analytical study of induced anisotropy in idealized granular materials. *Géotechnique* 1989;39(4):601–14.
- [46] Ruan B, Miao Y, Cheng K, Yao EL. Study on the small strain shear modulus of saturated sand-fines mixtures by bender element test. *European Journal of Environmental and Civil Engineering* 2018:1–11.
- [47] Ruedrich J, Bartelsen T, Dohrmann R, Siegesmund S. Moisture expansion as a deterioration factor for sandstone used in buildings. *Environ Earth Sci* 2011;63(7–8):1545–64.
- [48] Ruggeri P, Segato D, Fruzzetti VME, Scarpelli G. Evaluating the shear strength of a

- natural heterogeneous soil using reconstituted mixtures. *Géotechnique* 2016;66(11):941–6.
- [49] Shi XS, Herle I. Analysis of the compression behavior of artificial lumpy composite materials. *Int J Numer Anal Meth Geomech* 2016;40(10):1438–53.
- [50] Shi XS, Herle I, Muir Wood D. A consolidation model for lumpy composite soils in open-pit mining. *Géotechnique* 2018;68(3):189–204.
- [51] Shi XS, Yin J. Experimental and theoretical investigation on the compression behavior of sand-marine clay mixtures within homogenization framework. *Comput Geotech* 2017;90:14–26.
- [52] Shi XS, Zhao J, Yin J, Yu Z. An elastoplastic model for gap-graded soils based on homogenization theory. *Int J Solids Struct* 2019;163:1–14.
- [53] Shin H, Santamarina JC. Role of particle angularity on the mechanical behavior of granular mixtures. *J Geotech Geoenviron Eng* 2012;139(2):353–5.
- [54] Simoni A, Houlsby GT. The direct shear strength and dilatancy of sand-gravel mixtures. *Geotech Geol Eng* 2006;24(3):523.
- [55] Sivapullaiah PV, Sridharan A, Stalin VK. Hydraulic conductivity of bentonite-sand mixtures. *Can Geotech J* 2000;37(2):406–13.
- [56] Sufian A, Russell AR, Whittle AJ. Anisotropy of contact networks in granular media and its influence on mobilised internal friction. *Géotechnique* 2017;67(12):1067–80.
- [57] Sun Y, Nimbalkar S, Chen C. Grading and frequency dependence of the resilient modulus of ballast. *Geotech Lett* 2018;8(4):305–9.
- [58] Sun Y, Shen Y, Chen C. A grading parameter for evaluating the grading-dependence of the shear stiffness of granular aggregates. *Particuology* 2018;36:193–8.
- [59] Tan DY, Yin JH, Feng WQ, Zhu ZH, Qin JQ, Chen WB. New Simple Method for Calculating impact force on flexible barrier considering partial muddy debris flow passing through. *J Geotech Geoenviron Eng* 2019;145(9):04019051.
- [60] Tan SA, Karunaratne GP, Muhammad N. Sand penetration into clay slurry through jute interlayer. *Soils Found* 1994;34(2):19–25.
- [61] Tandon GP, Weng GJ. A theory of particle-reinforced plasticity. *J Appl Mech* 1988;55(1):126–35.
- [62] Vallejo LE. Interpretation of the limits in shear strength in binary granular mixtures. *Can Geotech J* 2001;38(5):1097–104.
- [63] Vallejo LE, Mawby R. Porosity influence on the shear strength of granular material-clay mixtures. *Eng Geol* 2000;58(2):125–36.
- [64] Wang X, Gong JA, Zhang K, Nie Z. Random generation of convex granule packing based on weighted Voronoi tessellation and cubic-polynomial-curve fitting. *Comput Geotech* 2019;113:103088.
- [65] Wichtmann T, Triantafyllidis T. Influence of the grain-size distribution curve of quartz sand on the small strain shear modulus  $G_{max}$ . *J Geotech Geoenviron Eng* 2009;135(10):1404–18.
- [66] Yao YP, Hou W, Zhou AN. UH model: three-dimensional unified hardening model for overconsolidated clays. *Géotechnique* 2009;59(5):451–69.
- [67] Yin JH. Properties and behavior of Hong Kong marine deposits with different clay contents. *Can Geotech J* 1999;36(6):1085–95.
- [68] Zeng LL, Cai YQ, Cui YJ, Hong ZS. Hydraulic conductivity of reconstituted clays based on intrinsic compression. *Géotechnique* 2019:1–8.
- [69] Zhang X, Baudet BA. Particle breakage in gap-graded soil. *Géotechnique Lett* 2013;3(2):72–7.
- [70] Zhang ZF, Ward AL, Keller JM. Determining the porosity and saturated hydraulic conductivity of binary mixtures. *Vadose Zone J* 2011;10(1):313–21.
- [71] Zhao J, Guo N. Unique critical state characteristics in granular media considering fabric anisotropy. *Géotechnique* 2013;63(8):695.
- [72] Zhao MH, Zou XJ, Zou PX. Disintegration characteristics of red sandstone and its filling methods for highway roadbed and embankment. *J Mater Civ Eng* 2007;19(5):404–10.
- [73] Zhao S, Evans TM, Zhou X. Effects of curvature-related DEM contact model on the macro-and micro-mechanical behaviours of granular soils. *Géotechnique* 2018;17:158.
- [74] Zhao S, Evans TM, Zhou X. Shear-induced anisotropy of granular materials with rolling resistance and particle shape effects. *Int J Solids Struct* 2018;150:268–81.
- [75] Zhou B, Huang R, Wang H, Wang J. DEM investigation of particle anti-rotation effects on the micromechanical response of granular materials. *Granul Matter* 2013;15(3):315–26.
- [76] Zhou B, Wang J, Wang H. A novel particle tracking method for granular sands based on spherical harmonic rotational invariants. *Géotechnique* 2018;68(12):1116–23.
- [77] Zhou B, Wang J, Wang H. Three-dimensional sphericity, roundness and fractal dimension of sand particles. *Géotechnique* 2018;68(1):18–30.
- [78] Zhou Y, Wang H, Zhou B, Li J. DEM-aided direct shear testing of granular sands incorporating realistic particle shape. *Granul Matter* 2018;20(3):55.
- [79] Zhou Z, Yang H, Wang X, Liu B. Model development and experimental verification for permeability coefficient of soil-rock mixture. *Int J Geomech* 2016;17(4):04016106.